Biomarker evidence of the water mass structure and primary productivity changes in the Chukchi Sea over the past 70 years

Chao Gao[1,2,3], Xiaoyan Ruan[4], Yi Ge Zhang[3], Huan Yang[2], Xiaotong Xiao[5], Xiaoxia Lü[2], Yi Yang[2]*, Hongmei Wang[2] and Xiaoguo Yu[6]*

[1]School of Earth Sciences, China University of Geosciences, Wuhan, China, [2]State Key Laboratory of Biogeology and Environmental Geology, China University of Geosciences, Wuhan, China, [3]Department of Oceanography, Texas A&M University, College Station, TX, United States, [4]Key Laboratory of Tectonics and Petroleum Resources of Ministry of Education, China University of Geosciences, Wuhan, China, [5]Frontiers Science Center for Deep Ocean Multispheres and Earth System, and Key Laboratory of Marine Chemistry Theory and Technology, Ministry of Education, Ocean University of China, Qingdao, China, [6]Key Laboratory of Submarine Geosciences & Second Institute of Oceanography, Ministry of Natural Resources, Hangzhou, China

The Chukchi Sea has experienced significant changes under global warming in the Common Era, including the shift of primary productivity. However, modern observations are too short to fully investigate the effects of environmental changes in this area. Here, we analyzed lipid biomarkers (e.g. long-chain *n*-alkanes, *n*-alkanols, *n*-alkanoic acids, diols, and sterols) from a sediment core (R07) collected from the Chukchi Sea shelf to determine phytoplankton primary productivity variations and factors influencing these changes over the past 70 years. Similar trends of the abundance of terrestrial ecosystem-derived compounds (e.g. long-chain *n*-alkanes, *n*-alkanols, *n*-alkanoic acids, and C_{32} 1,15-diol) indicate that terrigenous input increased from ca. 1946 towards ca. 1983 and then decreased thereafter. In comparison, biomarkers with marine origin indicate that the ratio of diatoms to dinoflagellates increased after ca. 1983 towards the core-top (ca. 2011). Concurrent changes in terrigenous input and phytoplankton community indicated a shift in water mass structure at ca. 1983 (i.e. the Alaska Coastal Water decreased and the Bering Sea Water increased), which may be attributed to the phase shift of the Arctic Oscillation and/or unsynchronized flow changes in different water masses. Owing to the different water mass properties, the change of water mass structure caused intense water mixing and the resulting high turbidity in the study area, which led to light limitation for phytoplankton growth. These conditions probably account for the reduced phytoplankton primary productivity from ca. 1983 to ca. 2000 in the general trend of increasing. The results indicate that, in addition to global warming and sea ice retreat, other factors, such as change in regional water mass structure (i.e. different water masses), may also have a significant influence on the primary productivity and the phytoplankton community in the Chukchi Sea shelf.

KEYWORDS

Chukchi Sea, Phytoplankton, Primary productivity, Water mass structure, Lipid biomarkers

1 Introduction

The Arctic Ocean is sensitive to global warming, exemplified by drastic changes in recent decades (Serreze and Barry, 2011). The most notable change is the summer sea ice decline, which continuously accelerated in recent years (Stroeve et al., 2012; Stroeve and Notz, 2018; Brennan et al., 2020). Satellite measurements show that the Arctic summer sea ice extent declined by more than 10% per decade between 1979 and 2010 (Stroeve et al., 2012). From 1979 to 2018, there is a 12 day earlier melt onset and 28 day later freeze-up for Arctic sea ice (Stroeve and Notz, 2018). And an ice-free Arctic Ocean during summer is predicted by the mid-century or sooner (Overland and Wang, 2013; IPCC, 2014).

Sea ice dynamics have been found to alter environment and phytoplankton primary productivity in the Arctic Ocean (Hunt et al., 2002; Grebmeier et al., 2006; Arrigo et al., 2008; Arrigo et al., 2014; Frey et al., 2014). A reduced sea ice extent produces large open areas that serve as habitats for phytoplankton growth, and prolonged open water duration favors the extension of the phytoplankton growing season (Arrigo et al., 2008; Pabi et al., 2008). Between 1998 and 2012, a significant increase (ca. 30%) in the annual net primary production across the Arctic Ocean has been reported, and this increase correlates with the mean open water area and length of the open water season (May–September) (Arrigo et al., 2008; Arrigo and van Dijken, 2015). Loss of sea ice on the shelf can improve light availability at the surface ocean, and thus enhance phytoplankton productivity (Arrigo and van Dijken, 2011; Winder et al., 2012; Hill et al., 2018). Further, ice thinning and melt ponds multiplication promote primary production under sea ice (Arrigo et al., 2014). As a consequence, net primary production in the Arctic Ocean is projected to continue to increase this century (Vancoppenolle et al., 2013).

However, nutrient availability is also a key factor controlling primary productivity which is related to land input and water mass location and structure (Popova et al., 2010; Lee et al., 2019; Terhaar et al., 2021), suggesting that production change of the Arctic Ocean in the future might not be a simple, monotonic increase as sea ice declines. It has been observed regions with similar sea ice conditions are yet characterized by different primary productivity in the Arctic Ocean (Grebmeier et al., 2006; Pabi et al., 2008; Arrigo and van Dijken, 2015; Zhuang et al., 2016; Giesbrecht et al., 2018). In addition, river discharge to the Arctic Ocean has been observed to increase during the past decades (Peterson et al., 2002; Ge et al., 2013; Zhang et al., 2013), which can bring more terrestrial materials and steer the primary production (Terhaar et al., 2021). The freshwater content has been reported to have an effect on phytoplankton primary production and phytoplankton community in the Chukchi Sea by controlling nutrient inventory (Pabi et al., 2008; Yun et al., 2014; Yun et al., 2016; Park et al., 2022). Phytoplankton comprises the base of the marine food web in the Arctic ecosystem. Therefore, establishing phytoplankton productivity and community structure and determining their environmental driving factors are critical for evaluating the long-term impacts of climate change on the Arctic marine ecosystem.

Because of the sampling difficulty in this harsh and often inaccessible environment in the Arctic Ocean, most of previous studies focused on field observations and satellite/remote sensing data, which are mainly restrained to the last 2-3 decades (e.g. Grebmeier et al., 2006; Pabi et al., 2008; Arrigo and van Dijken, 2015; Zhuang et al., 2016; Giesbrecht et al., 2018). The scarcity of long-term phytoplankton records hinders our understanding of controlling factors and related mechanisms in the Arctic Ocean ecosystem. But biomarkers found in marine sediment can help in resolving this problem. A substantial body of research indicates that lipid biomarkers can be utilized as effective tracers for reconstructing phytoplankton productivity and their community structures on different temporal scales. For example, brassicasterol, dinosterol, and C_{30} diols have been considered as the indicator of phytoplankton productivity, synthesized by diatoms, dinoflagellates, and eustigmatophytes, respectively (Schubert et al., 1998; Li et al., 2013; Punyu et al., 2014 and references therein). Several studies have used these source-specific compounds to explore the change of primary productivity and community structure in the Arctic Ocean and the adjacent seas (e.g. Belicka et al., 2004; Hu et al., 2020).

The Chukchi Sea shelf is characterized by high productivity, with an estimated annual integrated primary production ranging from 170 to 720 g C m^{-2} yr^{-1} (Hill et al., 2018). The burial of export productivity as well as land-derived carbon in the Chukchi Sea shelf makes it an important carbon sink (Gosselin et al., 1997; Grebmeier, 2012). As a marginal area of the Arctic Ocean, the Chukchi Sea shelf experienced significant environmental changes in recent years, e.g., reduced summer sea ice cover, increased sea surface temperature (SST) and altered Pacific inflow (Serreze et al., 2016; Woodgate, 2018). These changes affected environmental conditions, thereby promoting rapid shifts in ecosystem structures (Giesbrecht et al., 2018). Previous studies have emphasized sea ice, light, temperature, nutrients and their interactions exerting controls on primary productivity of the Chukchi Sea shelf (Hill et al., 2005; Doney, 2006; Arrigo et al., 2008; Winder and Sommer, 2012). Thus, the Chukchi Sea shelf represents an ideal area to investigate the response of phytoplankton to Arctic environmental changes. In this study, biomarkers in a sediment core from the Chukchi Sea shelf were analyzed to reconstruct variations of the primary productivity and community structure over the past ca. 70 years, substantially extending existing instrumental records. The temporal variations of biomarker abundance and ratios offer unique perspective of primary productivity changes of this area.

2 Regional setting

The Chukchi Sea has an area extent of 6.20×10^5 km^2 (Jakobsson, 2002), representing a shallow (average depth of 50 m) (Baskaran and Naidu, 1995) and seasonally ice-covered continental shelf of the Arctic Ocean (Grebmeier et al., 2006). Owing to the pressure-head difference between the Pacific and Arctic oceans, the annual average northward transportation of Pacific water through the Bering Strait to the Chukchi Sea is approximately 1.0 Sv (1×10^6 m^3/s), with the maximum (minimum) transport in summer (winter) (Woodgate et al., 2012; Woodgate, 2018). In the Chukchi Sea, the water masses from the Bering Sea bifurcate into the Alaskan Coastal Water (ACW) and Bering Sea Water (BSW) (Coachman et al., 1975; Hunt et al., 2013; Figure 1). The ACW originates from the south of the Aleutian Islands, and is augmented by river runoff (especially the Yukon River) from western Alaska (Steele et al., 2004). This nutrient-limited, warm (1℃< T< 6℃) and fresh (31‰ < salinity< 32‰) ACW flows along the coast of Alaska to Barrow Canyon (Steele et al., 2004). The BSW, which is relatively nutrient-rich, cold (summer temperature of 0℃ ~ 2℃) and saline (summer salinity of
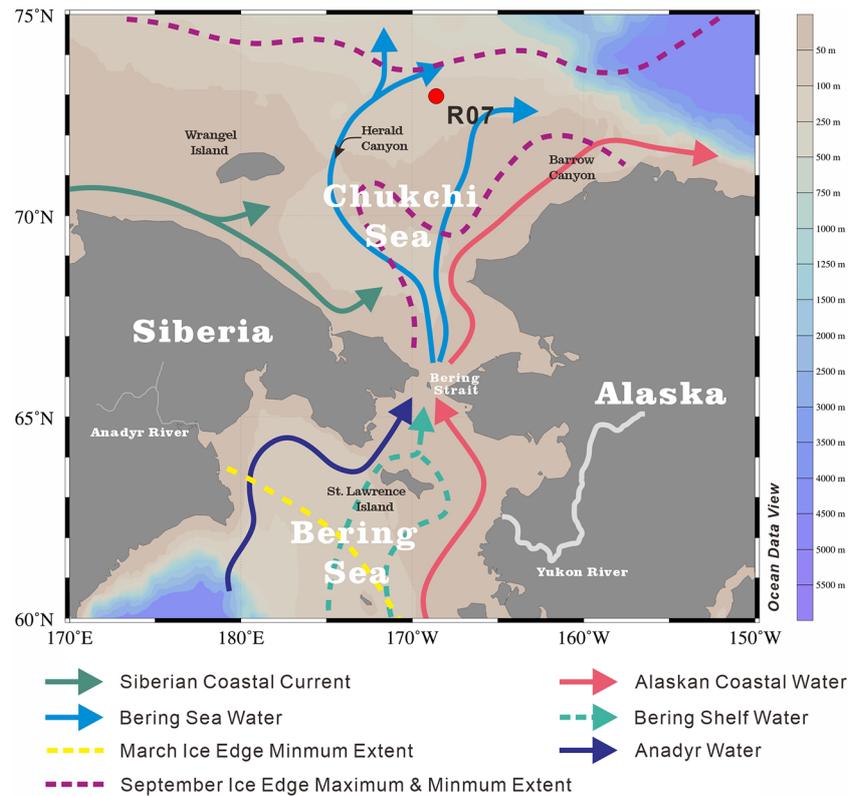
FIGURE 1

Location of our studied sediment core R07 (red dot) on Chukchi Sea shelf. Surface currents were modified from Grebmeier et al. (2006). The base map was generated with the Ocean Data View software (Schlitzer, 2016).

32‰ ~ 33‰), further splits into two branches during its northward flow (Steele et al., 2004; Hunt et al., 2013). One branch, with some mix into the ACW, continues flowing northward between shoals *via* the Central Channel (Steele et al., 2004; Weingartner et al., 2005), while the other branch mixes with the cold and fresh Siberian Coastal Current (Weingartner et al., 1999), and flows northwest into the Herald Valley to the east of the Wrangel Island (Coachman et al., 1975). After passing the Herald Valley, the water spreads northeastward to the north-central shelf and eastward along the north of the Herald Shoal (Weingartner et al., 2005). Carrying nutrients, heat and freshwater into the Chukchi Sea, these Pacific-origin water masses significantly impact biological and physical processes in the area (Hill et al., 2005; Weingartner et al., 2005; Grebmeier et al., 2006). For example, under the influence of these water masses, the nutrient concentration (nitrate, phosphate and silicate), salinity and temperature show distinctly different characteristics along the 73°N transect where the study core (R07) is located (Figure 2).

3 Material and methods

3.1 Sampling and dating

Sediment core R07 (28 cm long) was collected from the Chukchi Sea shelf (73.00°N, 168.97°W, 73 m water depth; Figure 1) with a multiple-core sampler during the sixth Chinese National Arctic Research Expeditions in 2014. The lithological characteristics have

been described in Zhang et al. (2018). Briefly, sediment core R07 was dominated by silt (avg. = 65%) and clay (avg. = 25%). The very top layer (0-1 cm) was used for other research, with the remaining core (1-28 cm) sampled every cm, and stored at –20°C until analysis.

^{210}Pb concentrations were measured to determine the chronology of Core R07 using ORTEC HPGe detectors (GEM, Lo-Ax and GMX) at the Nanjing Institute of Geography and Limnology, and had been published by Zhang et al. (2018). A sedimentation rate of 0.41 cm yr^{-1} (Zhang et al., 2018; Figure S1) was calculated using the constant initial concentration (CIC) model (Oldfield et al., 1978) for Core R07 (see supplementary material for details), which is similar to the sedimentation rate reported from an adjacent station (71.49°N, 167.78°W, 0.37 cm yr^{-1}, Cooper and Grebmeier, 2018) and also within the estimated range of 0.20-0.70 cm yr^{-1} sedimentation rate of the Chukchi Sea shelf (Huh et al., 1997). The ^{210}Pb results indicate the Core R07 contained an ca. 70-years sediment record (from ca. 1946 to ca. 2011).

3.2 Lipid analysis

Methods for biomarker analysis were modified from Yang et al. (2014). Briefly, an aliquot of each freeze-dried and homogenized sediment-sample (ca. 5 g) was ultrasonically extracted (×7) using a mixture of dichloromethane (DCM) and methanol (MeOH) (9:1, v:v). Dry sediments were spiked with known amounts of internal standards (androstane, cholan-24-oic acid, and androstan-3-ol) for
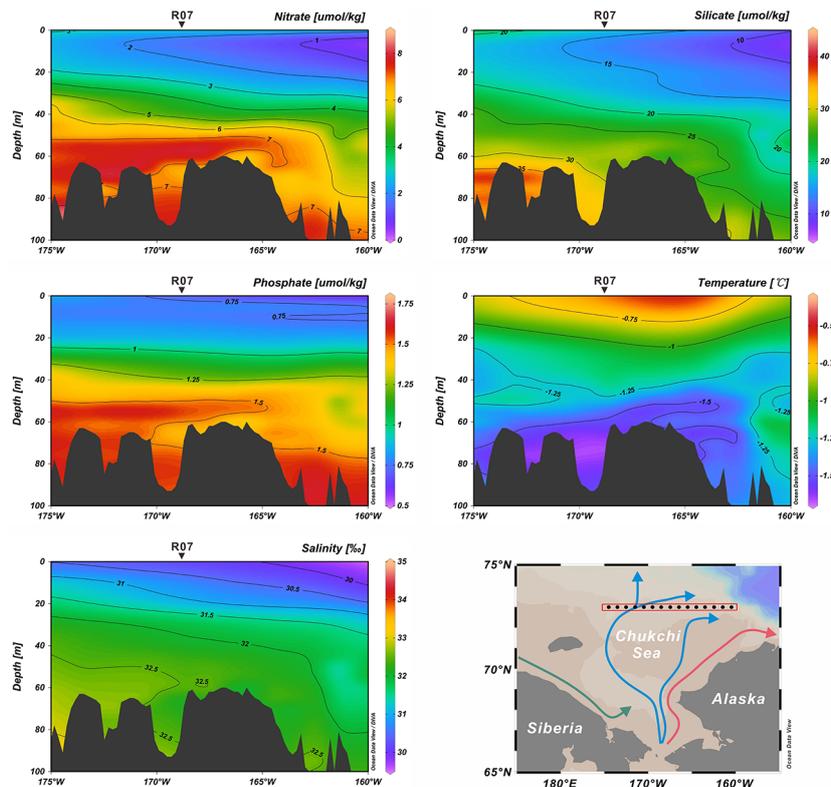
FIGURE 2
Annual vertical profiles of nitrate, silicate, phosphate, salinity and temperature along 73°N transect. These data were downloaded from WOA 2018 in the National Centers for Environmental Information (NCEI; https://www.ncei.noaa.gov/access/world-ocean-atlas-2018/).

biomarker quantification before lipid extraction. The total lipid extracts were separated into non-polar and polar fractions on silica gel chromatography columns by eluting with *n*-hexane and MeOH, respectively. After drying under a gentle stream of nitrogen gas, the non-polar fraction containing *n*-alkanes was redissolved for instrumental analysis, while the polar fraction was saponified with 5 mL of 1-mol/L KOH/MeOH (5% H_2O) solution for 2 h at 80 °C. After cooling, the solution was extracted using *n*-hexane (2 mL × 6) to obtain the neutral fraction, containing *n*-alkanols, sterols, diols, etc. The remaining solution was then acidified using HCl (pH< 2), and then extracted with *n*-hexane (2 mL × 6) to obtain the fatty acids. All fractions were dried under nitrogen gas, and the neutral fraction was derivatized using N, O-bis (trimethylsilyl)-trifluoroacetamide (BSTFA) at 70°C for 1.5 h. The fatty acids were esterified using a 14% BF_3/MeOH solution at 70°C for 1.5 h, and then extracted with *n*-hexane (2 mL × 6).

The alkanes, derivatized neutral compounds, and fatty acid methyl esters were analyzed using a gas chromatography-mass spectrometer (GC-MS; Agilent 7890A/5975C) equipped with a DB-5MS capillary column (60 m × 0.25 mm × 0.25 μm). The GC oven was heated from 70 to 210°C at 10°C/min, and from 210 to 310°C at 3°C/min, and then held at 310°C for 36 min, with helium as the carrier gas. The inlet temperature was 310°C and the EI energy was 70 eV. Samples were scanned in the full scan mode from 50 to 550 *m/z*.

Compounds were identified by comparing their mass spectra with literature (Boon et al., 1979; Volkman, 1986; Versteegh et al., 1997; Rampen et al., 2012) and database (NIST08 library data). Diols were

quantified in the extracted ion chromatogram according to Rampen et al. (2012). Concentrations of different compounds were calculated by comparing peak areas with those of internal standards and then normalized to the dry weights of sediments. It needs to be pointed out that since the potential response factor differences between compounds of interests and internal standards were not determined, the quantification results are considered semi-quantitative. However, this limitation should not affect our conclusions since we focused on variations of biomarker concentrations over time as well as their ratios.

The Carbon Preference Index (CPI) of *n*-alkanes was calculated using the following formula:

$$CPI_{25-33} = 1/2 * [(C_{25} + C_{27} + C_{29} + C_{31})/ \qquad (1)$$
$$(C_{26} + C_{28} + C_{30} + C_{32}) +$$
$$(C_{27} + C_{29} + C_{31} + C_{33})/$$
$$(C_{26} + C_{28} + C_{30} + C_{32})]$$

The CPI for *n*-alkanols and *n*-alkanoic acids were calculated using the following equation:

$$CPI_{22-30} = 1/2 * [(C_{22} + C_{24} + C_{26} + C_{28})/ \qquad (2)$$
$$(C_{23} + C_{25} + C_{27} + C_{29}) +$$
$$(C_{24} + C_{26} + C_{28} + C_{30})/$$
$$(C_{23} + C_{25} + C_{27} + C_{29})]$$

3.3 Environmental data

The original data of the monthly Arctic Oscillation (AO) index were obtained from National Oceanic and Atmospheric Administration (NOAA) Climate Prediction Center (https://www.cpc.ncep.noaa.gov/products/precip/CWlink/daily_ao_index/ao.shtml). Since phytoplankton growth in the Chukchi Sea shelf mainly occurs in summer (Hill et al., 2018; Bai et al., 2019), the summer AO index was calculated, which is an average of the AO index in June, July and August.

The historical SSTs at core R07 location were obtained from the NOAA Extended Reconstructed Sea Surface Temperature (ERSST) V5 (Huang et al., 2017), which is provided by the NOAA/OAR/ESRL PSD, Boulder, Colorado, USA (at https://www.esrl.noaa.gov/psd/data/gridded/data.noaa.ersst.v5.html). The SST calculation is described in detail by Gao et al. (2021). Considering the SST in winter (December, January and February, DJF) and spring (March, April and May, MAM) is –1.8°C, the SST of an average of summer (June, July and August, JJA) and fall (September, October and November, SON) is used in this paper.

Monthly satellite sea ice concentration (SIC) data (1979–2020) were downloaded from Nimbus-7 SMMR and DMSP SSM/I-SSMIS Passive Microwave Data at the National Snow and Ice Data Center (NSIDC, http://nsidc.org/data, grid cell size 25 × 25 km; Cavalieri et al., 1996). As the area where R07 core is located is covered by sea ice in winter (DJF) and spring (MAM) (SIC=100%) (Figure S2), which corresponds to the SST –1.8°C, an average SIC of summer (JJA) and fall (SON) were used in this study. Although satellite SIC data before 1979 is absent, we can get the SIC record before 1979 from the SST data the significant correlation between SIC and SST during 1979 to 2020 (Figure S3; see supplementary material for details).

Sea water temperature, salinity and nutrients (nitrate, silicate and phosphate) at different depth were downloaded from World Ocean Atlas (WOA) 2018 in the National Centers for Environmental Information (NCEI) on a 1° grid resolution (https://www.ncei.noaa.gov/access/world-ocean-atlas-2018/). These databases provide standardized vertical intervals from the surface (0 m) to the seafloor (5500 m) with annual mean parameters between 1955 and 2017. Parameter values at 0, 10, 20, 30, 50, 75 and 100 m were used in this paper. The data for the 73°N transect where R07 core is located were calculated by averaging the 72.5°N and 73.5°N transect (Figure 2).

SST and SIC in this paper represent the average values of SST and SIC in summer (JJA) and fall (SON), respectively.

4 Results

n-Alkanes, n-alkanols, n-alkanoic acids, sterols, and diols are present in all samples (Table S1). The concentrations of long-chain n-alkanes (C_{25}-C_{33}) in core R07 vary from 3.00 to 4.28 µg/g downcore, while the concentrations of long-chain n-alkanoic acids (C_{24}-C_{30}) and long-chain n-alkanols (C_{24}-C_{30}) range from 5.60 to 9.49 µg/g (Figure 3C), and from 6.37 to 10.95 µg/g (Figure 3D), respectively. The long-chain n-alkanes with odd carbon number are dominant ($CPI_{25\text{-}33}$ = 3.80-4.25, with an average of 4.03 for n = 27), whereas even carbon number compounds dominate among high

molecular weight n-alkanols ($CPI_{22\text{-}30}$ = 2.59-3.62, with an average of 3.23 for n = 27) and n-alkanoic acids ($CPI_{22\text{-}30}$ = 6.37-10.95, with an average of 8.38 for n = 27). C_{32} 1,15-diol concentrations vary between 94.40-150.00 ng/g (Figure 3E). The abundance of long-chain n-alkanes, n-alkanols, n-alkanoic acids, and C_{32} 1,15-diol in Core R07 exhibit similar trends, i.e., they increase from ca. 1946 towards ca. 1983, and then decrease from ca. 1983 towards the present (Figure 3).

Biomarkers derived from phytoplankton (brassicasterol, dinosterol, and C_{30} diols) were also identified and quantified (Table S1). Brassicasterol concentration ranged from 0.36 to 2.14 µg/g, whereas dinosterol abundance varied from 0.46 to 1.19 µg/g, and C_{30} diols (C_{30} 1,13- and C_{30} 1,15-diol) concentration ranged from 0.16 to 0.33 µg/g. These biomarkers show similar trends in Core R07, i.e., they were increasing from ca. 1946 towards ca. 1983 and from ca. 2000 towards ca. 2011, and decreasing between the two periods (from ca. 1983 to ca. 2000) (Figure 4). As an indicator of relative changes in diatoms and dinoflagellates, the brassicasterol/dinosterol (B/D) ratio ranged from 0.74 to 1.80, with an average of 0.99 before ca. 1983, and of 1.53 thereafter (Figure 3A).

5 Discussion

5.1 Sources and significance of biomarkers in the core samples

Long-chain n-alkanes, n-alkanols, and n-alkanoic acids are ubiquitous in marine sediments, which have been widely employed as an indicator of terrestrial input in marine environments (Eglinton and Eglinton, 2008; Naeher et al., 2022). In Core R07, the distribution characteristics (high CPI) of long-chain n-alkanes, n-alkanols, and n-alkanoic acids indicate that these compounds are derived from terrestrial plants (Eglinton and Hamilton, 1967; Rielley et al., 1991; Meyers, 1997; Eglinton and Eglinton, 2008). Some bacteria could also contain long-chain n-alkanes; however, these n-alkanes lack an odd-over-even carbon predominance, with low CPI values of approximately 1.0 (Han and Calvin, 1969; Cranwell et al., 1987). In Arctic Ocean, these compounds have been used to reconstruct terrigenous input into sediments (Belicka et al., 2004; Yunker et al., 2005; Faux et al., 2011; Yunker et al., 2011) and sediment trap material (Bai et al., 2019).

C_{32} 1,15-diol, a tracer for the riverine input (Lattaud et al., 2017a; Lattaud et al., 2017b; Lattaud et al., 2019), was also detected in Core R07. C_{32} 1,15-diol is mainly produced by freshwater eustigmatophytes in rivers (Lattaud et al., 2017a) and transported to the continental shelf by currents. Previous studies have shown that the Chukchi Sea shelf receives high amounts of sediments from rivers (especially Yukon River) (Stein, 2008; Darby et al., 2009), which probably explains the presence of C_{32} 1,15-diol in Core R07.

Interestingly, the concentrations of terrigenous biomarkers, including long-chain n-alkanes, n-alkanols, n-alkanoic acids, and C_{32} 1,15-diol, exhibit similar trends in Core R07 (Figure 3). Previous studies showed that the terrestrial materials in the Arctic Ocean sediment were transported to this area mainly through sea ice and water mass (or current) (Belicka et al., 2002; Belicka et al., 2009; Darby et al., 2009; Stein, 2019). Sea ice contains terrigenous material and release it to the area of sea-ice melting (Stein, 2019). But, there is
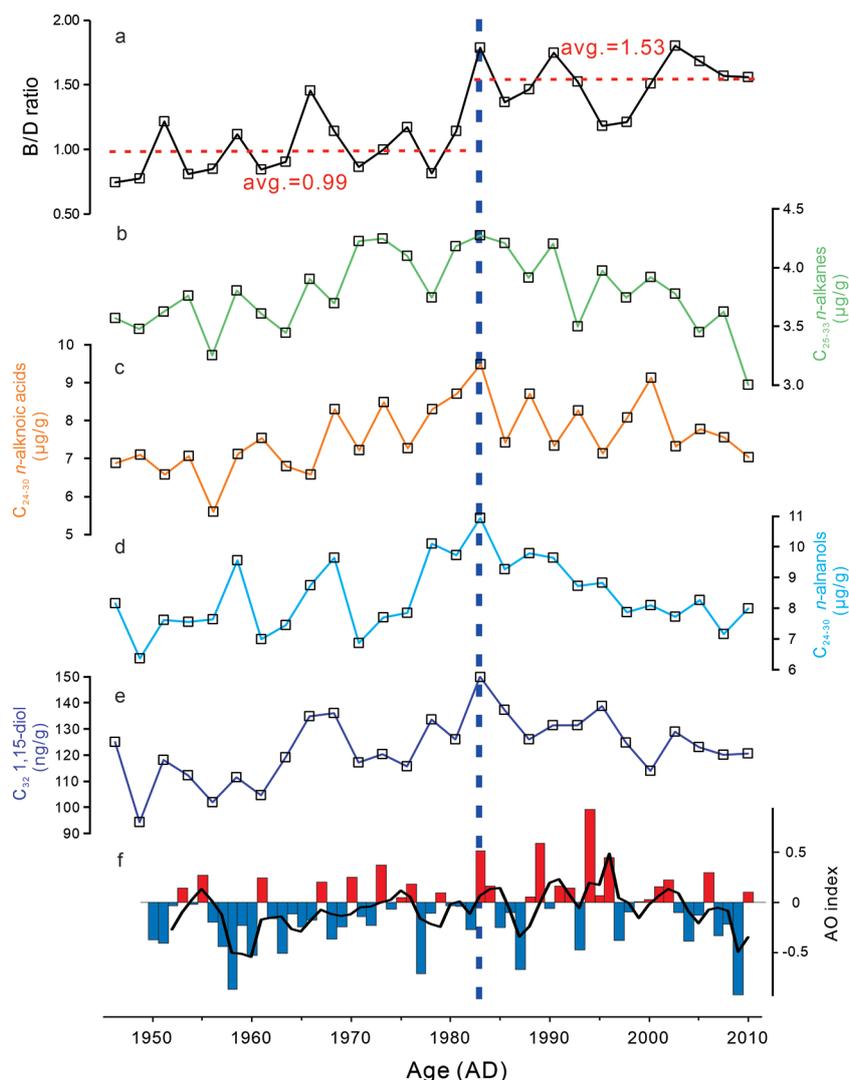
FIGURE 3
Temporal variations in brassicasterol/dinosterol (B/D) ratio, concentrations of long-chain *n*-alkanes, *n*-alkanols, *n*-alkanoic acids, and C$_{32}$ 1,15-diol in the R07 core, and summer AO index. Red (blue) bar in AO index indicates positive (negative) value, and black line represents the 3-years running mean. The AO index data were obtained from NOAA Climate Prediction Center (https://www.cpc.ncep.noaa.gov/products/precip/CWlink/daily_ao_index/ao.shtml).

no significant change in SIC before and after 1983 (Figure 4), indicated by SST (Figure S4; mean SST of –0.92°C for 1974~1983 and –0.78°C for 1984~1993). Thus, this synchronous change in terrigenous input is unlikely to be caused by the sea ice. Considering that C$_{32}$ 1,15-diol is derived from riverine input, the similar trend of terrigenous compounds indicates that changes in the contribution of riverine input, which was transported mainly by water mass to this area, may primarily account for the variations in concentrations of these biomarkers in Core R07. This was supported by the year-round sediment trap from the Chukchi Sea. Their results showed that the mass fluxes of long-chain *n*-alkanes started increase with the sea ice melt, and the highest occurred during the ice free period (Bai et al., 2019), when there is the highest river discharge (Ge et al., 2013).

Abundant marine ecosystem-derived compounds were also detected in Core R07, including brassicasterol (24-methylcholesta-5,22E-dien-3β-ol), dinosterol (4α,23,24-trimethyl-5α-cholest-22-en-3β-ol), and C$_{30}$ diols, which are thought to be biomarkers for

diatoms, dinoflagellates, and eustigmatophytes, respectively, and their concentrations can reflect the corresponding phytoplankton productivity (Schubert et al., 1998; He et al., 2013). Although brassicasterol can be produced by algae other than diatoms, such as dinoflagellates and haptophytes (Volkman, 1986; Ding et al., 2019), in an ecosystem dominated by diatoms, this compound is mainly produced by diatoms and could be used for reconstructing the diatom productivity (Wu et al., 2016; Wang et al., 2019). In the Chukchi Sea shelf, the phytoplankton community was dominated by diatoms, which account for at least 60% of the total population (Sergeeva et al., 2010; Lewis et al., 2019). Although brassicasterol and dinosterol also have terrigenous sources, they are thought to be generally minor in open ocean waters (Volkman, 1986; Fahl and Stein, 1999). In addition, considering the small percentage of terrestrial organic matter as indicated by low branched and isoprenoid tetraethers (BIT) index values (avg. = 0.07; Gao et al., 2021) and high $δ^{13}C_{org}$ (avg. = –22.25‰; Zhang et al., 2018), these brassicasterol and dinosterol in R07 should be mainly from marine algae. Thus,

FIGURE 4
Temporal variations in concentrations of brassicasterol, dinosterol, and C_{30} diols, TOC from R07, and SST/SIC at the study area. a. TOC from Zhang et al. (2018); b. The blue solid line represents the download satellite SIC data, and the blue dash line represents the SIC data calculated based on SST. The satellite SIC data are from the National Snow and Ice Data Center (NSIDC; Cavalieri et al., 1996). Historical SST data were obtained from the NOAA ERSST V5 (https://www.esrl.noaa.gov/psd/data/gridded/data.noaa.ersst.v5.html; Huang et al., 2017).

brassicasterol, dinosterol and C_{30} diols can represent the production of diatom, dinoflagellate, and eustigmatophytes, respectively. In Core R07, concentrations of these biomarkers showed similar trend and were roughly consistent with the changes in TOC (Figure 4).

Although quantifying the contribution of individual phytoplankton productivity with biomarkers is difficult at present due to lipid biosynthesis per cell differing among species (Ding et al., 2019), source-specific compounds (biomarker) are useful for evaluating relative changes in the biomass of different phytoplankton (Bi et al., 2021). For example, the B/D ratio enables assessment of spatiotemporal changes in the relative concentrations of diatoms and dinoflagellates, and subsequent, paleoenvironmental reconstruction at different timescales (Schubert et al., 1998; He et al., 2013; Wu et al., 2016 and references therein).

Degradation can influence biomarker concentrations in marine sediments, thereby complicating their utilization in paleoenvironment studies (Hernández-Sánchez et al., 2014; Naeher et al., 2022). However, the shallow water depth (73 m), high primary production, and high deposition rate in this area (Grebmeier et al., 2006) enable a high fraction of the algae-derived organic matters to reach the sediments (Belicka et al., 2002). In addition, the temperature in Chukchi Sea shelf water are relatively low, which is beneficial for lipid preservation. In Core R07, lipid concentrations do not exhibit a single decreasing trend from the top to bottom (Figures 3, 4), which is different from the typical degradation distribution. Therefore, biomarkers in sediments from Core R07 are unlikely to be considerably affected by degradation or diagenetic processes, and can, therefore, reflect the original input.

5.2 Water mass structure changes in the Chukchi Sea shelf

In Core R07, the B/D ratios showed different pattern, with an average value of 0.99 before ca. 1983, and of 1.53 after then (Figure 3A), indicating a change in the phytoplankton community (increased proportion of diatoms relative to dinoflagellates). Owing to differences in the optimal growth environments of phytoplankton, the phytoplankton community structure was influenced by water physical conditions and nutrient concentrations, which were significantly affected by the location and structure of water mass (Figure 2; Springer and McRoy, 1993; Lee et al., 2007). Therefore, phytoplankton community is considered to be water mass-specific (Hamilton et al., 2008; Sergeeva et al., 2010; Zhuang et al., 2016; Martini et al., 2016; Giesbrecht et al., 2018; Lee et al., 2019). According to previous study in the western Chukchi Sea shelf, there is more dinoflagellates relative to diatoms in the area close to ACW than that close to BSW (Sergeeva et al., 2010). In particular, observed data showed that spread of the ACW reduced the diatom biomass in the Chukchi Sea (Zhuang et al., 2016). Thus, the change in phytoplankton community recorded by the elevated B/D ratios in Core R07, which indicates an increased diatoms relative to dinoflagellates (Figure 3A) highlight water mass structure change in this area, i.e., reduced ACW and increased BSW.

Relative to the ACW, the BSW is colder, saltier, and richer in nutrients (Figure 2; Woodgate, 2018), and these properties are beneficial for water mixing. It has been reported that, compared with dinoflagellates, diatoms are reported to bloom at colder temperatures, higher nutrients, and intense mixing conditions (Margalef, 1978; Winder and Sommer, 2012; Xiao et al., 2018). Laboratory experiments (diatom-dinoflagellate competition experiments) also showed that there is a competitive superiority of the diatoms at high nutrient concentration, low temperature and low N:P ratios (Bi et al., 2021). In addition, as essential substance for diatom growth, high silicate favors the diatom growth has been reported in natural environments (Ragueneau et al., 2002; Allen et al., 2005) and incubation experiment (Lü et al., 2020). As the WOA data showed, in the area that close to the ACW (east of the R07), there is lower nitrate, lower silicate and higher temperature (Figure 2). Thus, the altered water condition associated with reduced ACW enhanced the growth of diatoms relative to dinoflagellates and thereby increasing the B/D ratio (Figure 3A).

Change in seasonal sea ice is another important factor affecting phytoplankton community structure, which has been reported in different area in Arctic Ocean, such as Chukchi Sea (Fujiwara et al., 2016; Neeley et al., 2018), Bering Sea (Fujiwara et al., 2016), Canada Basin (Coupel et al., 2012) and East Siberian Seas (Lee et al., 2019). However, the constant SIC before and after 1983 in the study area (Figure 4; Figure S4) indicates that change in phytoplankton community structure in R07 is unlikely to be caused by sea ice change.

The change in water mass structure is also reflected in the terrigenous input variations in Core R07, which reveals synchronous change with the phytoplankton community (Figure 3). The concentrations of terrestrial biomarkers (i.e., long-chain n-alkanes, n-alkanols, n-alkanoic acids, C_{32} 1,15-diol) were used to trace the terrestrial input into the Chukchi Sea, considering that end-member proxies, such as BIT (Hopmans et al., 2004), $\delta^{13}C_{org}$ (Naidu

et al., 1993) and C/N (Middelburg and Nieuwenhuize, 1998), are influenced by changes in marine organic matters. In R07, these terrigenous biomarkers showed increasing trends since ca. 1946 (Figure 3), which indicate the increased terrestrial input. As indicated in Section 5.1, variations in the biomarker concentrations in Core R07 are primarily caused by changes in riverine input that was transported to this area. The Yukon River is among the six largest rivers in the Arctic region (Cooper et al., 2008), and plays a particularly important role in the supply of terrestrial organic matter into the Chukchi Sea (Stein, 2008; Darby et al., 2009; Harvey and Taylor, 2017). The estimated annual freshwater discharge of the Yukon River is approximately 205 km³, with a suspended matter flux of 5.4×10^7 t (Stein, 2008). According to previous studies, river discharge to the Arctic Ocean is increasing since 1940s (Peterson et al., 2002; Wu et al., 2005), in particular, the discharge records at Pilot Station showed an increasing trend of Yukon River discharge (Ge et al., 2013). Increased river discharge from the Yukon River and others along the Alaska coast is entrained in the ACW and transported northward into the Chukchi Sea (Mathis et al., 2005; Iken et al., 2010), thereby elevating the terrestrial organic matter input, as depicted in Core R07 before ca. 1983 (Figure 3).

However, under the increasing riverine input, terrigenous input indicated by terrestrial biomarkers showed a decreasing trend after ca. 1983 (Figure 3), which may be attributed to changes in the structure of the water mass. Previous studies showed that the ACW plays a central role in transporting terrestrial materials into the Chukchi Sea shelf (Naidu et al., 2004; Harvey and Taylor, 2017; Zhang et al., 2021). With the change in water mass structure, i.e., reduced ACW in this area, the terrestrial organic matter input transported by the ACW to the study area significantly decreased. Consequently, the concentrations of terrestrial-derived organic matter reduced since ca. 1983 (Figure 3).

The change in water mass structure is likely to be associated with a phase shift in the AO and/or unsynchronized flow changes in the ACW and BSW. The AO is an annular mode of atmospheric circulation, with an annular (circled) center covering the entire Arctic region (Thompson and Wallace, 1998; Wang et al., 2014). AO-derived wind anomaly is cyclonic and anticyclonic during the positive and negative phases, respectively (Figure S5; Proshutinsky and Johnson, 1997; Wu et al., 2006; Wang et al., 2014). It has been reported that wind can change the surface distribution of water masses in the Chukchi Sea (Winsor and Chapman, 2004). With the summer AO shift to a predominantly positive phase at approximately 1983 (Figure 3A), a cyclonic wind anomaly occurred and caused a westerly wind anomaly in the Chukchi Sea shelf (Figure S5). Derived by the westerly wind anomaly, the ACW moved eastward since ca. 1983, thereby reducing its impact on the Core R07 area (Figure 2).

However, after the predominant phase of AO shift from positive to negative after ca. 2003, there is still elevated B/D ratios and decreasing trend in terrigenous biomarker (Figure 3), which may be attributed to the unsynchronized changes in the ACW and BSW. Mooring data showed that there was an increase in the annual mean transport of BSW into the Arctic at least since 2002, whereas no evident trend for the annual mean flow of the ACW (Woodgate, 2018). The unsynchronized changes in water masses also can cause the elevated proportion of BSW and the reduced impact of ACW in the Core R07 area. However, since these mooring data are only

available from 2002, it is uncertain whether the structure change of water mass at ca. 1983 was caused by the asynchronous change. In addition, considering the complexity of this area, more research is needed to explore the exact processes and factors of changes in water mass structure.

5.3 Primary productivity changes in the Chukchi Sea shelf over the last 70 years

In the Arctic Ocean, phytoplankton production was controlled by the extreme seasonality of the polar environment (Nelson et al., 2014). Stimulated by increasing irradiance, the annual phytoplankton growth starts with ice algae at the ice-water interface (Gradinger, 2009). As the sea ice thins and retreats in the spring or summer, light availability gradually increases to be sufficient to trigger the blooms of under-ice phytoplankton, which has been observed beneath the 0.8- to 1.3-m-thick sea ice in the Chukchi Sea shelf (Arrigo et al., 2012). This under-ice phytoplankton bloom was also found in Core R07. Low but significant amounts of phytoplankton biomarkers (avg. of 0.47 µg/g, 0.51µg/g and 178.63 ng/g for barssicasterol, dinosterol and C30 diols, respectively) were detected in sediments deposited during ca. 1946 to ca. 1953 when SST was –1.8°C and SIC was almost 100% (i.e. sea ice cover) throughout the year (Figure 4). As sea ice continues to melt, high phytoplankton productivity can last until the nutrient in water is depleted or the ice cover forms. A one-year sediment trap experiment conducted in the Chukchi Sea (DM: 74.6°N, 158.23°W) showed that phytoplankton biomarkers (brassicasterol and dinosterol) fluxes begin to rise as the sea ice melts and fall back to low levels before nutrient depletion or ice cover formation (Bai et al., 2019). Annual sea ice pattern in the area of R07 is similar with that of DM, i.e. sea ice starts to melt in June, and is completely formed in December (Figure S1), indicating similar growth patterns of phytoplankton between areas of R07 and DM. Besides, the subsurface phytoplankton blooms and near-bottom blooms have been observed in the Chukchi Sea shelf (Lowry et al., 2015; Stabeno et al., 2020), which might also occur in the area of Core R07.

In recent decades, the Arctic Ocean has undergone drastic changes, including an unprecedented warming (Serreze and Barry, 2011) and accelerated seasonal sea ice retreat (Stroeve et al., 2012). In the study area, SST showed an increasing trend and SIC was decreasing from 1952 (Figure 4), which indicated an earlier sea ice melting and, therefore, longer growth season for phytoplankton (Arrigo et al., 2008; Arrigo and van Dijken, 2015). As discussed in Section 5.2, the discharge from the Yukon River into the ACW increased in the past decades (Peterson et al., 2002; Ge et al., 2013). The increased terrestrial material transported by ACW elevated the terrigenous organic matter and nutrients into the study area (Figure 3), which are favorable for phytoplankton growth (Terhaar et al., 2021). Consequently, under the influence of increased temperature, longer growth season and increased terrigenous input, phytoplankton primary productivity in the Chukchi Sea shelf significantly increased, as reflected by the dramatic increase in marine-sourced lipids in Core R07 from ca. 1946 (Figure 4).

However, with the constant or slightly increased temperature between ca. 1983 to ca. 2000, there is a significant decrease in marine-sourced lipids, which is approximately half of the increase from ca. 1946 to ca. 1983 (Figures 4, S6), indicating a nonnegligible decrease in phytoplankton primary productivity. Similar changes also were found in a sediment core collected approximately 150 km south of Core R07, in which cyst density of a dinoflagellate species exhibited a significant decrease after a period of increase (Natsuike et al., 2013). We speculate that this decrease in phytoplankton productivity is likely caused by the change in the water mass structure, which has been suggested can impacts both the phytoplankton community and phytoplankton productivity (Grebmeier et al., 2006). As proposed by previous studies, primary productivity is controlled by the interaction of light and nutrients (Popova et al., 2010; Terhaar et al., 2021). As indicated in Section 5.2, there was a change in water mass structure at ca. 1983; more specifically, the contribution from the ACW decreased, while that from BSW increased. Compared to the ACW, BSW is colder and saltier (Grebmeier et al., 2006), and these characteristics of cold and salt accelerate water mixing, and consequently, increase turbidity. Light limitation induced by high turbidity has been reported to decrease productivity in the East China Sea and South Yellow Sea (Wu et al., 2016), Southern Ocean MIZ (Fitch and Moore, 2007), and coastal waters surrounding Qatar (Arabian Gulf) (Quigg et al., 2013). A similar phenomenon may also exist in the Chukchi Sea, as the enhancement experiments have showed that light is an important controlling factor for the phytoplankton productivity rates in this area (Lee et al., 2013). Notwithstanding that the AO shift led to an increase in nutrient-rich BSW in this area (Figure 2), nutrients might not be the main limiting factor of primary productivity as its minimal effect on primary productivity rates under high nutrient concentrations (Lee et al., 2013). In addition, high turbidity can reduce water transparency and thus diminish the light intensity reaching deep water layers, which may hinder or attenuate subsurface and near-bottom blooms. Thus, light limitation caused by change in water mass structure may decrease the phytoplankton productivity in the water column, as reflected by the decreased concentrations of marine biomarkers in Core R07 (Figure 4). This result suggests that, in addition to global warming and sea ice retreat, other factors (such as change in water mass structure) significantly affect phytoplankton primary productivity in the Chukchi Sea shelf.

Following the decrease, the biomarker concentrations in R07 showed significant increase in phytoplankton primary productivity since ca. 2000, which may be attributed to the warming and accelerated sea ice loss (Figure 4; Budikova, 2009; Stroeve et al., 2012). Warming enhances stratification and lowers the mixing depth, and both conditions increase light availability (Winder and Sommer, 2012). The higher SST and decreased SIC indicate a longer growth season for phytoplankton. In general, the primary production rates in open waters are significantly higher than those below snow-covered sea ice because of higher light intensities (Mathis et al., 2014). Longer phytoplankton growing season, increased light availability, and high nutrient content have been reported to increase primary production in the Arctic (Arrigo et al., 2008; Arrigo and van Dijken, 2015). Owing to these changes, the productivity of diatoms, dinoflagellates, and eustigmatophytes based on biomarkers increased from ca. 2000 to ca. 2011 in the Core R07 (Figure 4). The result is consistent with the increase in the

annual net primary production (42%) in the Chukchi Sea shelf from 1998 to 2012 (Arrigo and van Dijken, 2015).

6 Conclusions

Biomarkers for marine algae and terrestrial organic matter in Core R07 were quantified and used to investigate the changes in the environment and primary productivity in the Chukchi Sea shelf over the past 70 years. The nearly simultaneous changes in the phytoplankton community and terrigenous input indicate a change in the water mass structure at ca. 1983, i.e. decreased Alaska Coastal Water and increased Being Sea Water, which we attributed to an AO shift and/or unsynchronized changes in different water masses. Primary productivity reconstructed using biomarkers concentration in Core R07 generally increased with global warming and sea ice retreat. However, it significantly decreased from ca. 1983 to ca. 2000, probably because of increased intense water mixing and light limitation which were caused by the change in water mass structure. The findings indicate that primary productivity in the Chukchi Sea shelf is not only associated with global warming and sea ice retreat, but also influenced by other factors, such as change in water mass structure. Further exploration and understanding of the relationships between these factors and primary productivity changes in the Arctic Ocean at different time scales will enhance understanding of the responses of Arctic ecosystems to climate change.

Data availability statement

The original contributions presented in the study are included in the article/Supplementary Material. Further inquiries can be directed to the corresponding authors.

Author contributions

CG, YY and XY contributed to conception and design of the study. CG performed the experiments. CG, XR, YY and XY analyzed the data and wrote the first draft of the manuscript. YZ, HY, XX, XL and HW edited and polished the manuscript. All authors contributed to the article and approved the submitted version.

Conflict of interest

The authors declare that the research was conducted in the absence of any commercial or financial relationships that could be construed as a potential conflict of interest.

Publisher's note

All claims expressed in this article are solely those of the authors and do not necessarily represent those of their affiliated organizations, or those of the publisher, the editors and the reviewers. Any product that may be evaluated in this article, or claim that may be made by its manufacturer, is not guaranteed or endorsed by the publisher.

Supplementary material

The Supplementary Material for this article can be found online at: https://www.frontiersin.org/articles/10.3389/fmars.2023.1077656/full#supplementary-material

References

Allen, J. T., Brown, L., Sanders, R., Mark Moore, C., Mustard, A., Fielding, S., et al. (2005). Diatom carbon export enhanced by silicate upwelling in the northeast Atlantic. *Nature* 437 (7059), 728–732. doi: 10.1038/nature03948

Arrigo, K. R., Perovich, D. K., Pickart, R. S., Brown, Z. W., van Dijken, G. L., Lowry, K. E., et al. (2012). Massive phytoplankton blooms under Arctic sea ice. *Science* 336 (6087), 1408–1408. doi: 10.1126/science.1215065

Arrigo, K. R., Perovich, D. K., Pickart, R. S., Brown, Z. W., van Dijken, G. L., Lowry, K. E., et al. (2014). Phytoplankton blooms beneath the sea ice in the Chukchi sea. *Deep Sea Res. Part II: Topical Stud. Oceanogr* 105, 1–16. doi: 10.1016/j.dsr2.2014.03.018

Arrigo, K. R., and van Dijken, G. L. (2011). Secular trends in Arctic Ocean net primary production. *J. Geophys Research: Oceans* 116, C09011. doi: 10.1029/2011JC007151

Arrigo, K. R., and van Dijken, G. L. (2015). Continued increases in Arctic Ocean primary production. *Prog. Oceanogr* 136, 60–70. doi: 10.1016/j.pocean.2015.05.002

Arrigo, K. R., van Dijken, G., and Pabi, S. (2008). Impact of a shrinking arctic ice cover on marine primary production. *Geophys Res. Lett.* 35, L19603. doi: 10.1029/2008GL035028

Bai, Y., Sicre, M.-A., Chen, J., Klein, V., Jin, H., Ren, J., et al. (2019). Seasonal and spatial variability of sea ice and phytoplankton biomarker flux in the Chukchi sea (western Arctic Ocean). *Prog. Oceanogr* 171, 22–37. doi: 10.1016/j.pocean.2018.12.002

Baskaran, M., and Naidu, A. S. (1995). ^{210}Pb derived chronology and the fluxes of ^{210}Pb and ^{137}Cs isotopes into continental shelf sediments, East Chukchi Sea, Alaskan Arctic. *Geochimica Cosmochimica Acta* 59 (21), 4435–4448. doi: 10.1016/0016-7037(95)00248-X

Belicka, L. L., Macdonald, R. W., and Harvey, H. R. (2002). Sources and transport of organic carbon to shelf, slope, and basin surface sediments of the Arctic Ocean. *Deep Sea Res. Part I Oceanogr Res. Papers* 49 (8), 1463–1483. doi: 10.1016/S0967-0637(02)00031-6

Belicka, L. L., Macdonald, R. W., and Harvey, H. R. (2009). Trace element and molecular markers of organic carbon dynamics along a shelf–basin continuum in sediments of the western Arctic Ocean. *Mar. Chem.* 115 (1), 72–85. doi: 10.1016/j.marchem.2009.06.007

Belicka, L. L., Macdonald, R. W., Yunker, M. B., and Harvey, H. R. (2004). The role of depositional regime on carbon transport and preservation in Arctic Ocean sediments. *Mar. Chem.* 86 (1), 65–88. doi: 10.1016/j.marchem.2003.12.006

Bi, R., Cao, Z., Ismar-Rebitz, S. M. H., Sommer, U., Zhang, H., Ding, Y., et al. (2021). Responses of marine diatom-dinoflagellate competition to multiple environmental drivers: Abundance, elemental, and biochemical aspects. *Front. Microbiol.* 12 (2498). doi: 10.3389/fmicb.2021.731786

Boon, J. J., Rijpstra, W. I. C., De Lange, F., De Leeuw, J. W., Yoshioka, M., and Shimizu, Y. (1979). Black Sea sterol–a molecular fossil for dinoflagellate blooms. *Nature* 277 (5692), 125–127. doi: 10.1038/277125a0

Brennan, M. K., Hakim, G. J., and Blanchard-Wrigglesworth, E. (2020). Arctic Sea-Ice variability during the instrumental era. *Geophys Res. Lett.* 47 (7), e2019GL086843. doi: 10.1029/2019GL086843

Budikova, D. (2009). Role of Arctic sea ice in global atmospheric circulation: A review. *Global Planetary Change* 68 (3), 149–163. doi: 10.1016/j.gloplacha.2009.04.001

Cavalieri, D., Parkinson, C., Gloersen, P., and Zwally, H. (1996). *Sea Ice concentrations from nimbus-7 SMMR and DMSP SSM/I-SSMIS passive microwave data, version 1 (updated yearly)* (Boulder, Colorado USA: NASA National Snow and Ice Data Center Distributed Active Archive Center).

Coachman, L. K., Aagaard, K., and Tripp, R. B. (1975). *Bering Strait: The Regional Physical Oceanography.* University of Washington Press, 172.

Cooper, L. W., and Grebmeier, J. M. (2018). Deposition patterns on the Chukchi shelf using radionuclide inventories in relation to surface sediment characteristics. *Deep Sea Res. Part II: Topical Stud. Oceanogr* 152, 48–66. doi: 10.1016/j.dsr2.2018.01.009

Cooper, L. W., McClelland, J. W., Holmes, R. M., Raymond, P. A., Gibson, J., Guay, C. K., et al. (2008). Flow-weighted values of runoff tracers (δ^{18}O, DOC, ba, alkalinity) from the six largest Arctic rivers. *Geophys Res. Lett.* 35, L18606. doi: 10.1029/2008GL035007.

Coupel, P., Jin, H. Y., Joo, M., Horner, R., Bouvet, H. A., Sicre, M. A., et al. (2012). Phytoplankton distribution in unusually low sea ice cover over the pacific Arctic. *Biogeosciences* 9 (11), 4835–4850. doi: 10.5194/bg-9-4835-2012

Cranwell, P. A., Eglinton, G., and Robinson, N. (1987). Lipids of aquatic organisms as potential contributors to lacustrine sediments–II. *Organic Geochem* 11 (6), 513–527. doi: 10.1016/0146-6380(87)90007-6

Darby, D. A., Ortiz, J., Polyak, L., Lund, S., Jakobsson, M., and Woodgate, R. A. (2009). The role of currents and sea ice in both slowly deposited central Arctic and rapidly deposited Chukchi-Alaskan margin sediments. *Global Planetary Change* 68 (1), 58–72. doi: 10.1016/j.gloplacha.2009.02.007

Ding, Y., Bi, R., Sachs, J., Chen, X., Zhang, H., Li, L., et al. (2019). Lipid biomarker production by marine phytoplankton under different nutrient and temperature regimes. *Organic Geochem* 131, 34–49. doi: 10.1016/j.orggeochem.2019.01.008

Doney, S. C. (2006). Plankton in a warmer world. *Nature* 444 (7120), 695–696. doi: 10.1038/444695a

Eglinton, T. I., and Eglinton, G. (2008). Molecular proxies for paleoclimatology. *Earth Planetary Sci. Lett.* 275 (1), 1–16. doi: 10.1016/j.epsl.2008.07.012

Eglinton, G., and Hamilton, R. J. (1967). Leaf epicuticular waxes. *Science* 156 (3780), 1322–1335. doi: 10.1126/science.156.3780.1322

Fahl, K., and Stein, R. (1999). Biomarkers as organic-carbon-source and environmental indicators in the Late Quaternary Arctic Ocean: problems and perspectives. *Mar. Chem.* 63 (3), 293–309. doi: 10.1016/S0304-4203(98)00068-1

Faux, J. F., Belicka, L. L., and Harvey, H. R. (2011). Organic sources and carbon sequestration in Holocene shelf sediments from the western Arctic Ocean. *Continental Shelf Res.* 31 (11), 1169–1179. doi: 10.1016/j.csr.2011.04.001

Fitch, D. T., and Moore, J. K. (2007). Wind speed influence on phytoplankton bloom dynamics in the Southern Ocean Marginal Ice Zone. *J. Geophys Research: Oceans* 112, C08006. doi: 10.1029/2006JC004061

Frey, K. E., Maslanik, J. A., Clement Kinney, J., and Maslowski, W. (2014). "Recent variability in Sea ice cover, age, and thickness in the pacific Arctic region," in *The pacific Arctic region: Ecosystem status and trends in a rapidly changing environment*. Eds. J. M. Grebmeier and W. Maslowski (Dordrecht: Springer Netherlands), 31–63.

Fujiwara, A., Hirawake, T., Suzuki, K., Eisner, L., Imai, I., Nishino, S., et al. (2016). Influence of timing of sea ice retreat on phytoplankton size during marginal ice zone bloom period in the Chukchi and Bering shelves. *Biogeosciences* 12 (15), 12611–12651. doi: 10.5194/bg-13-115-2016

Gao, C., Yang, Y., Yang, H., Zhang, Y. G., Lü, X., Wang, H., et al. (2021). Different temperature dependence of marine-derived brGDGT isomers in a sediment core from the Chukchi Sea shelf. *Organic Geochem* 152, 104169. doi: 10.1016/j.orggeochem.2020.104169

Ge, S., Yang, D., and Kane, D. L. (2013). Yukon River basin long-term, (1977–2006) hydrologic and climatic analysis. *Hydrological Processes* 27 (17), 2475–2484. doi: 10.1002/hyp.9282

Giesbrecht, K. E., Varela, D. E., Wiktor, J., Grebmeier, J. M., Kelly, B., and Long, J. E. (2018). A decade of summertime measurements of phytoplankton biomass, productivity and assemblage composition in the pacific Arctic region from 2006 to 2016. *Deep Sea Res. Part II: Topical Stud. Oceanogr* 162, 93–113. doi: 10.1016/j.dsr2.2018.06.010

Gosselin, M., Levasseur, M., Wheeler, P. A., Horner, R. A., and Booth, B. C. (1997). New measurements of phytoplankton and ice algal production in the Arctic Ocean. *Deep Sea Res. Part II Topical Stud. Oceanogr* 44 (8), 1623–1644. doi: 10.1016/S0967-0645(97)00054-4

Gradinger, R. (2009). Sea-Ice algae: Major contributors to primary production and algal biomass in the Chukchi and Beaufort Seas during May/June 2002. *Deep Sea Res. Part II: Topical Stud. Oceanogr* 56 (17), 1201–1212.

Grebmeier, J. M. (2012). Shifting patterns of life in the pacific Arctic and Sub-Arctic seas. *Annu. Rev. Mar. Sci.* 4, 63–78. doi: 10.1146/annurev-marine-120710-100926

Grebmeier, J. M., Cooper, L. W., Feder, H. M., and Sirenko, B. I. (2006). Ecosystem dynamics of the pacific-influenced northern Bering and Chukchi Seas in the Amerasian Arctic. *Prog. Oceanogr* 71, 331–361. doi: 10.1016/j.pocean.2006.10.001

Hamilton, A. K., Lovejoy, C., Galand, P. E., and Ingram, R. G. (2008). Water masses and biogeography of picoeukaryote assemblages in a cold hydrographically complex system. *Limnology Oceanogr* 53 (3), 922–935. doi: 10.4319/lo.2008.53.3.0922

Han, J., and Calvin, M. (1969). Hydrocarbon distribution of algae and bacteria, and microbiological activity in sediments. *Proc. Natl. Acad. Sci. United States America* 64 (2), 436–443. doi: 10.1073/pnas.64.2.436

Harvey, H. R., and Taylor, K. A. (2017). Alkane and polycyclic aromatic hydrocarbons in sediments and benthic invertebrates of the northern Chukchi Sea. *Deep Sea Res. Part II: Topical Stud. Oceanogr* 144, 52–62. doi: 10.1016/j.dsr2.2017.08.011

Hernández-Sánchez, M. T., LaRowe, D. E., Deng, F., Homoky, W. B., Browning, T. J., Martin, P., et al. (2014). Further insights into how sediment redox status controls the preservation and composition of sedimentary biomarkers. *Organic Geochem* 76, 220–234. doi: 10.1016/j.orggeochem.2014.08.006

He, J., Zhao, M., Wang, P., Li, L., and Li, Q. (2013). Changes in phytoplankton productivity and community structure in the northern South China Sea during the past 260ka. *Palaeogeogr Palaeoclimatol Palaeoecol.* 392, 312–323. doi: 10.1016/j.palaeo.2013.09.010

Hill, V., Ardyna, M., Lee, S. H., and Varela, D. E. (2018). Decadal trends in phytoplankton production in the pacific Arctic region from 1950 to 2012. *Deep Sea Res. Part II: Topical Stud. Oceanogr* 152, 82–94. doi: 10.1016/j.dsr2.2016.12.015

Hill, V., Cota, G., and Stockwell, D. (2005). Spring and summer phytoplankton communities in the Chukchi and Eastern Beaufort seas. *Deep Sea Res. Part II: Topical Stud. Oceanogr* 52 (24), 3369–3385. doi: 10.1016/j.dsr2.2005.10.010

Hopmans, E. C., Weijers, J. W., Schefuß, E., Herfort, L., Sinninghe Damsté, J. S., and Schouten, S. (2004). A novel proxy for terrestrial organic matter in sediments based on branched and isoprenoid tetraether lipids. *Earth Planetary Sci. Lett.* 224 (1), 107–116. doi: 10.1016/j.epsl.2004.05.012

Huang, B., Thorne, P., Banzon, V., Boyer, T., Chepurin, G., Lawrimore, J., et al. (2017). Extended Reconstructed Sea Surface Temperature version 5 (ERSSTv5): Upgrades, validations, and intercomparisons. *Journal of Climate* 30(20), 8179–8205. doi: 10.1175/JCLI-D-16-0836.1

Huh, C.-A., Pisias, N. G., Kelley, J. M., Maiti, T. C., and Grantz, A. (1997). Natural radionuclides and plutonium in sediments from the western Arctic Ocean: sedimentation rates and pathways of radionuclides. *Deep Sea Res. Part II: Topical Stud. Oceanogr* 44 (8), 1725–1743. doi: 10.1016/S0967-0645(97)00040-4

Hu, L., Liu, Y., Xiao, X., Gong, X., Zou, J., Bai, Y., et al. (2020). Sedimentary records of bulk organic matter and lipid biomarkers in the Bering Sea: A centennial perspective of sea-ice variability and phytoplankton community. *Mar. Geology* 429, 106308. doi: 10.1016/j.margeo.2020.106308

Hunt, G. L.Jr, Blanchard, A. L., Boveng, P., Dalpadado, P., Drinkwater, K. F., Eisner, L., et al. (2013). The Barents and Chukchi Seas: Comparison of two Arctic shelf ecosystems. *J. Mar. Syst.* 109-110, 43–68. doi: 10.1016/j.jmarsys.2012.08.003

Hunt, G. L.Jr, Stabeno, P., Walters, G., Sinclair, E., Brodeur, R. D., Napp, J. M., et al. (2002). Climate change and control of the southeastern Bering Sea pelagic ecosystem. *Deep Sea Res. Part II: Topical Stud. Oceanogr* 49 (26), 5821–5853. doi: 10.1016/S0967-0645(02)00321-1

Iken, K., Bluhm, B., and Dunton, K. (2010). Benthic food-web structure under differing water mass properties in the southern Chukchi Sea. *Deep Sea Res. Part II: Topical Stud. Oceanogr* 57 (1), 71–85. doi: 10.1016/j.dsr2.2009.08.007

IPCC (2014). *Climate change 2013: the physical science basis: Working group I contribution to the fifth assessment report of the intergovernmental panel on climate change* (Cambridge: Cambridge University press).

Jakobsson, M. (2002). Hypsometry and volume of the Arctic Ocean and its constituent seas. *Geochem Geophysics Geosystems* 3 (5), 1–18. doi: 10.1029/2001GC000302

Lattaud, J., Dorhout, D., Schulz, H., Castañeda, I. S., Schefuß, E., Damsté, J. S. S., et al. (2017b). The C32 alkane-1,15-diol as a proxy of late quaternary riverine input in coastal margins. *Climate Past* 13, 1049–1061. doi: 10.5194/cp-13-1049-2017

Lattaud, J., Kim, J.-H., De Jonge, C., Zell, C., Sinninghe Damsté, J. S., and Schouten, S. (2017a). The C32 alkane-1,15-diol as a tracer for riverine input in coastal seas. *Geochimica Cosmochimica Acta* 202, 146–158. doi: 10.1016/j.gca.2016.12.030

Lattaud, J., Lo, L., Zeeden, C., Liu, Y.-J., Song, S.-R., van der Meer, M. T. J., et al. (2019). A multiproxy study of past environmental changes in the Sea of Okhotsk during the last 1.5 Ma. *Organic Geochem* 132, 50–61. doi: 10.1016/j.orggeochem.2019.04.003

Lee, Y., Min, J.-O., Yang, E. J., Cho, K.-H., Jung, J., Park, J., et al. (2019). Influence of sea ice concentration on phytoplankton community structure in the Chukchi and East Siberian Seas, pacific Arctic Ocean. *Deep Sea Res. Part I: Oceanogr Res. Papers* 147, 54–64. doi: 10.1002/2016JC011977

Lee, S. H., Whitledge, T. E., and Kang, S.-H. (2007). Recent carbon and nitrogen uptake rates of phytoplankton in Bering Strait and the Chukchi Sea. *Continental Shelf Res.* 27 (17), 2231–2249. doi: 10.1016/j.csr.2007.05.009

Lee, S. H., Yun, M. S., Kim, B. K., Saitoh, S.-I., Kang, C.-K., Kang, S.-H., et al. (2013). Latitudinal carbon productivity in the Bering and Chukchi Seas during the summer in 2007. *Continental Shelf Res.* 59, 28–36. doi: 10.1016/j.csr.2013.04.004

Lewis, K. M., Arntsen, A. E., Coupel, P., Joy-Warren, H., Lowry, K. E., Matsuoka, A., et al. (2019). Photoacclimation of Arctic Ocean phytoplankton to shifting light and nutrient limitation. *Limnology Oceanogr* 64 (1), 284–301. doi: 10.1002/lno.11039

Li, L., Li, Q., Tian, J., Wang, H., and Wang, P. (2013). Low latitude hydro-climatic changes during the Plio-Pleistocene: evidence from high resolution alkane records in the

southern South China Sea. *Quaternary Sci. Rev.* 78, 209–224. doi: 10.1016/j.quascirev.2013.08.007

Lowry, K. E., Pickart, R. S., Mills, M. M., Brown, Z. W., van Dijken, G. L., Bates, N. R., et al. (2015). The influence of winter water on phytoplankton blooms in the Chukchi Sea. *Deep Sea Res. Part II: Topical Stud. Oceanogr* 118, 53–72. doi: 10.1016/j.dsr2.2015.06.006

Lü, J.-J., Zhang, G.-T., and Zhao, Z.-X. (2020). Seawater silicate fertilizer facilitated nitrogen removal *via* diatom proliferation. *Mar. pollut. Bull.* 157, 111331. doi: 10.1016/j.marpolbul.2020.111331

Margalef, R. (1978). Life-forms of phytoplankton as survival alternatives in an unstable environment. *Oceanol. Acta* 1 (4), 493–509.

Martini, K. I., Stabeno, P. J., Ladd, C., Winsor, P., Weingartner, T. J., Mordy, C. W., et al. (2016). Dependence of subsurface chlorophyll on seasonal water masses in the Chukchi Sea. *J. Geophys Research: Oceans* 121 (3), 1755–1770. doi: 10.1002/2015JC011359

Mathis, J. T., Grebmeier, J. M., Hansell, D. A., Hopcroft, R. R., Kirchman, D. L., Lee, S. H., et al. (2014). "Carbon biogeochemistry of the Western Arctic: Primary production, carbon export and the controls on Ocean acidification," in *The pacific Arctic region: Ecosystem status and trends in a rapidly changing environment* (Dordrecht: Springer Netherlands), 223–268.

Mathis, J. T., Hansell, D. A., and Bates, N. R. (2005). Strong hydrographic controls on spatial and seasonal variability of dissolved organic carbon in the Chukchi Sea. *Deep Sea Res. Part II: Topical Stud. Oceanogr* 52 (24), 3245–3258. doi: 10.1016/j.dsr2.2005.10.002

Meyers, P. A. (1997). Organic geochemical proxies of paleoceanographic, paleolimnologic, and paleoclimatic processes. *Organic Geochem* 27 (5), 213–250. doi: 10.1016/S0146-6380(97)00049-1

Middelburg, J. J., and Nieuwenhuize, J. (1998). Carbon and nitrogen stable isotopes in suspended matter and sediments from the Schelde Estuary. *Mar. Chem.* 60 (3), 217–225. doi: 10.1016/S0304-4203(97)00104-7

Naeher, S., Cui, X., and Summons, R. E. (2022). Biomarkers: Molecular tools to study life, environment, and climate. *Elements* 18 (2), 79–85. doi: 10.2138/gselements.18.2.79

Naidu, A., Cooper, L., Grebmeier, J., Whitledge, T., Hameedi, M., Stein, R., et al. (2004). "The continental margin of the north Bering-Chukchi Sea: concentrations, sources, fluxes, accumulation and burial rates of organic carbon," in *The organic carbon cycle in the Arctic Ocean* (Berlin: Springer), 193–203.

Naidu, A. S., Scalan, R. S., Feder, H. M., Goering, J. J., Hameedi, M. J., Parker, P. L., et al. (1993). Stable organic carbon isotopes in sediments of the north Bering-south Chukchi Seas, Alaskan-Soviet Arctic Shelf. *Continental Shelf Res.* 13 (5-6), 669–691. doi: 10.1016/0278-4343(93)90099-J

Natsuike, M., Nagai, S., Matsuno, K., Saito, R., Tsukazaki, C., Yamaguchi, A., et al. (2013). Abundance and distribution of toxic alexandrium tamarense resting cysts in the sediments of the Chukchi Sea and the eastern Bering Sea. *Harmful Algae* 27, 52–59. doi: 10.1016/j.hal.2013.04.006

Neeley, A. R., Harris, L. A., and Frey, K. E. (2018). Unraveling phytoplankton community dynamics in the northern Chukchi Sea under sea-ice-covered and sea-ice-free conditions. *Geophys Res. Lett.* 45 (15), 7663–7671. doi: 10.1029/2018GL077684

Nelson, R. J., Ashjian, C. J., Bluhm, B. A., Conlan, K. E., Gradinger, R. R., Grebmeier, J. M., et al. (2014). "Biodiversity and biogeography of the lower trophic taxa of the pacific Arctic region: Sensitivities to climate change," in *The pacific Arctic region: Ecosystem status and trends in a rapidly changing environment* (Dordrecht: Springer Netherlands), 269–336.

Oldfield, F., Appleby, P. G., and Battarbee, R. W. (1978). Alternative ^{210}Pb dating: results from the new Guinea highlands and lough erne. *Nature* 271 (5643), 339–342. doi: 10.1038/271339a0

Overland, J. E., and Wang, M. (2013). When will the summer Arctic be nearly sea ice free? *Geophys Res. Lett.* 40, 2097–2101. doi: 10.1002/grl.50316

Pabi, S., van Dijken, G. L., and Arrigo, K. R. (2008). Primary production in the Arctic Ocean, 1998-2006. *J. Geophys Research: Oceans* 113, C08005. doi: 10.1029/2007JC004578

Park, J.-W., Kim, Y., Kim, K.-W., Fujiwara, A., Waga, H., Kang, J. J., et al. (2022). Contribution of small phytoplankton to primary production in the northern Bering and Chukchi seas. *Water* 14 (2), 235. doi: 10.3390/w14020235

Peterson, B. J., Holmes, R. M., McClelland, J. W., Vörösmarty, C. J., Lammers, R. B., Shiklomanov, A. I., et al. (2002). Increasing river discharge to the Arctic Ocean. *Science* 298 (5601), 2171–2173. doi: 10.1126/science.1077445

Popova, E., Yool, A., Coward, A., Aksenov, Y., Alderson, S., De Cuevas, B., et al. (2010). Control of primary production in the Arctic by nutrients and light: insights from a high resolution Ocean general circulation model. *Biogeosciences* 7 (11), 3569–3591. doi: 10.5194/bg-7-3569-2010

Proshutinsky, A. Y., and Johnson, M. A. (1997). Two circulation regimes of the wind-driven Arctic Ocean. *J. Geophys Research: Oceans* 102, 12493–12514. doi: 10.1029/97JC00738

Punyu, V. R., Banakar, V. K., and Garg, A. (2014). Equatorial Indian Ocean productivity during the last 33 kyr and possible linkage to Westerly Jet variability. *Mar. Geology* 348, 44–51. doi: 10.1016/j.margeo.2013.11.010

Quigg, A., Al-Ansi, M., Al Din, N. N., Wei, C.-L., Nunnally, C. C., Al-Ansari, I. S., et al. (2013). Phytoplankton along the coastal shelf of an oligotrophic hypersaline environment in a semi-enclosed marginal sea: Qatar (Arabian gulf). *Continental Shelf Res.* 60, 1–16. doi: 10.1016/j.csr.2013.04.015

Ragueneau, O., Chauvaud, L., Leynaert, A., Thouzeau, G., Paulet, Y.-M., Bonnet, S., et al. (2002). Direct evidence of a biologically active coastal silicate pump: Ecological implications. *Limnology Oceanogr* 47 (6), 1849–1854. doi: 10.4319/lo.2002.47.6.1849

Rampen, S. W., Willmott, V., Kim, J. H., Uliana, E., Mollenhauer, G., Schefuß, E., et al. (2012). Long chain 1,13- and 1,15-diols as a potential proxy for palaeotemperature reconstruction. *Geochimica Cosmochimica Acta* 84 (84), 204–216. doi: 10.1016/j.gca.2012.01.024

Rielley, G., Collier, R. J., Jones, D. M., and Eglinton, G. (1991). The biogeochemistry of Ellesmere lake, U.K.–I: source correlation of leaf wax inputs to the sedimentary lipid record. *Organic Geochem* 17 (6), 901–912. doi: 10.1016/0146-6380(91)90031-E

Schlitzer, R. (2016). *Ocean data view*. Available at: http://odv.awi.de.

Schubert, C. J., Villanueva, J., Calvert, S. E., Cowie, G. L., Rad, U. V., Schulz, H., et al. (1998). Stable phytoplankton community structure in the Arabian Sea over the past 200,000 years. *Nature* 394 (6693), 563–566. doi: 10.1038/29047

Sergeeva, V. M., Sukhanova, I. N., Flint, M. V., Pautova, L. A., Grebmeier, J. M., and Cooper, L. W. (2010). Phytoplankton community in the Western Arctic in July–august 2003. *Oceanology* 50 (2), 184–197. doi: 10.1134/S0001437010020049

Serreze, M. C., and Barry, R. G. (2011). Processes and impacts of Arctic amplification: A research synthesis. *Global Planetary Change* 77 (1), 85–96. doi: 10.1016/j.gloplacha.2011.03.004

Serreze, M. C., Crawford, A. D., Stroeve, J., Barrett, A. P., and Woodgate, R. A. (2016). Variability, trends, and predictability of seasonal sea ice retreat and advance in the Chukchi Sea. *J. Geophys Res.* 121 (10), 7308–7325. doi: 10.1002/2016JC011977

Springer, A. M., and McRoy, C. P. (1993). The paradox of pelagic food webs in the northern Bering Sea–III. patterns of primary production. *Continental Shelf Res.* 13 (5-6), 575–599. doi: 10.1016/0278-4343(93)90095-F

Stabeno, P. J., Mordy, C. W., and Sigler, M. F. (2020). Seasonal patterns of near-bottom chlorophyll fluorescence in the eastern Chukchi Sea: 2010–2019. *Deep Sea Res. Part II: Topical Stud. Oceanogr* 177, 104842. doi: 10.1016/j.dsr2.2020.104842

Steele, M., Morison, J., Ermold, W., Rigor, I., Ortmeyer, M., and Shimada, K. (2004). Circulation of summer pacific halocline water in the Arctic Ocean. *J. Geophys Res. Oceans* 109 (C2), 235–250. doi: 10.1029/2003JC002009

Stein, R. (2008). *Arctic Ocean sediments: Processes, proxies, and paleoenvironment* (Amsterdam: Elsevier).

Stein, R. (2019). The late Mesozoic-Cenozoic Arctic Ocean climate and sea ice history: A challenge for past and future scientific Ocean drilling. *Paleoceanogr Paleoclimatol* 34 (12), 1851–1894. doi: 10.1029/2018PA003433

Stroeve, J., and Notz, D. (2018). Changing state of Arctic sea ice across all seasons. *Environ. Res. Lett.* 13 (10), 103001. doi: 10.1088/1748-9326/aade56

Stroeve, J. C., Serreze, M. C., Holland, M. M., Kay, J. E., Malanik, J., and Barrett, A. P. (2012). The arctic's rapidly shrinking sea ice cover: a research synthesis. *Climatic Change* 110 (3-4), 1005–1027. doi: 10.1007/s10584-011-0101-1

Terhaar, J., Lauerwald, R., Regnier, P., Gruber, N., and Bopp, L. (2021). Around one third of current Arctic Ocean primary production sustained by rivers and coastal erosion. *Nat. Commun.* 12 (1), 169. doi: 10.1038/s41467-020-20470-z

Thompson, D. W. J., and Wallace, J. M. (1998). The Arctic Oscillation signature in the wintertime geopotential height and temperature fields. *Geophys Res. Lett.* 25 (9), 1297–1300. doi: 10.1029/98GL00950

Vancoppenolle, M., Bopp, L., Madec, G., Dunne, J., Ilyina, T., Halloran, P. R., et al. (2013). Future Arctic Ocean primary productivity from CMIP5 simulations: Uncertain outcome, but consistent mechanisms. *Global Biogeochem Cycles* 27 (3), 605–619. doi: 10.1002/gbc.20055

Versteegh, G. J. M., Bosch, H. J., and Leeuw, J. W. D. (1997). Potential palaeoenvironmental information of C_{24} to C_{36} mid-chain diols, keto-ols and mid-chain hydroxy fatty acids; a critical review. *Organic Geochem* 27 (1), 1–13. doi: 10.1016/S0146-6380(97)00063-6

Volkman, J. K. (1986). A review of sterol markers for marine and terrigenous organic matter. *Organic Geochem* 9 (2), 83–99. doi: 10.1016/0146-6380(86)90089-6

Wang, J., Eicken, J., Yu, Y., Bai, X., Zhang, J., Hu, H., et al. (2014). Abrupt climate changes and emerging ice-ocean processes in the Pacific Arctic Region and the Bering Sea. In: J. M. Grebmeier and W. Maslowski (Eds.), *The Pacific Arctic Region: Ecosystem Status and Trends in a Rapidly Changing Environment*. Springer, Dordrecht, pp. 65–99.

Wang, Z., Xiao, X., Yuan, Z., Wang, F., Xing, L., Gong, X., et al. (2019). Air-sea interactive forcing on phytoplankton productivity and community structure changes in the East China Sea during the Holocene. *Global Planetary Change* 179, 80–91. doi: 10.1016/j.gloplacha.2019.05.008

Weingartner, T., Aagaard, K., Woodgate, R., Danielson, S., Sasaki, Y., and Cavalieri, D. (2005). Circulation on the north central Chukchi Sea shelf. *Deep Sea Res. Part II: Topical Stud. Oceanogr* 52 (24-26), 3150–3174. doi: 10.1016/j.dsr2.2005.10.015

Weingartner, T. J., Danielson, S., Sasaki, Y., Pavlov, V., and Kulakov, M. (1999). The Siberian Coastal Current: A wind- and buoyancy-forced Arctic coastal current. *J. Geophys Research: Oceans* 104 (C12), 29697–29713. doi: 10.1029/1999jc900161

Winder, M., Berger, S. A., Lewandowska, A., Aberle, N., Lengfellner, K., Sommer, U., et al. (2012). Spring phenological responses of marine and freshwater plankton to changing temperature and light conditions. *Mar. Biol.* 159 (11), 2491–2501. doi: 10.1007/s00227-012-1964-z

Winder, M., and Sommer, U. (2012). Phytoplankton response to a changing climate. *Hydrobiologia* 698 (1), 5–16. doi: 10.1007/s10750-012-1149-2

Winsor, P., and Chapman, D. C. (2004). Pathways of pacific water across the Chukchi Sea: A numerical model study. *J. Geophys Research: Oceans* 109 (C3), C03002. doi: 10.1029/2003JC001962

Woodgate, R. A. (2018). Increases in the pacific inflow to the Arctic from 1990 to 2015, and insights into seasonal trends and driving mechanisms from year-round Bering Strait mooring data. *Prog. Oceanogr* 160, 124–154. doi: 10.1016/j.pocean.2017.12.007

Woodgate, R. A., Weingartner, T. J., and Lindsay, R. (2012). Observed increases in Bering strait Oceanic fluxes from the pacific to the Arctic from 2001 to 2011 and their impacts on the Arctic Ocean water column. *Geophys Res. Lett.* 39 (24), L24603. doi: 10.1029/2012GL054092

Wu, P., Bi, R., Duan, S., Jin, H., Chen, J., Hao, Q., et al. (2016). Spatiotemporal variations of phytoplankton in the East China Sea and the yellow Sea revealed by lipid biomarkers. *J. Geophys Research: Biogeosciences* 121 (1), 109–125. doi: 10.1002/2015JG003167

Wu, B., Wang, J., and Walsh, J. E. (2006). Dipole Anomaly in the winter Arctic atmosphere and its association with sea ice motion. *J. Climate* 19 (2), 210–225. doi: 10.1175/JCLI3619.1

Wu, P., Wood, R., and Stott, P. (2005). Human influence on increasing Arctic river discharges. *Geophys Res. Lett.* 32, L02703. doi: 10.1029/2004GL021570

Xiao, W., Liu, X., Irwin, A. J., Laws, E. A., Wang, L., Chen, B., et al. (2018). Warming and eutrophication combine to restructure diatoms and dinoflagellates. *Water Res.* 128, 206–216. doi: 10.1016/j.watres.2017.10.051

Yang, H., Ding, W. H., and Xie, S. C. (2014). Distribution of microbial fatty acids and fatty alcohols in soils from an altitude transect of Mt. Jianfengling in Hainan, China: Implication for paleoaltimetry and paleotemperature reconstruction. *Sci. China: Earth Sci.* 57 (5), 999–1012. doi: 10.1007/s11430-013-4729-8

Yunker, M. B., Belicka, L. L., Harvey, H. R., and Macdonald, R. W. (2005). Tracing the inputs and fate of marine and terrigenous organic matter in Arctic Ocean sediments: A multivariate analysis of lipid biomarkers. *Deep-Sea Res. Part II* 52 (24), 3478–3508. doi: 10.1016/j.dsr2.2005.09.008

Yunker, M. B., Macdonald, R. W., Snowdon, L. R., and Fowler, B. R. (2011). Alkane and PAH biomarkers as tracers of terrigenous organic carbon in Arctic Ocean sediments. *Organic Geochem* 42 (9), 1109–1146. doi: 10.1016/j.orggeochem.2011.06.007

Yun, M. S., Whitledge, T. E., Kong, M., and Lee, S. H. (2014). Low primary production in the Chukchi Sea shelf, 2009. *Continental Shelf Res.* 76, 1–11. doi: 10.1016/j.csr.2014.01.001

Yun, M. S., Whitledge, T. E., Stockwell, D., Son, S. H., Lee, J. H., Park, J. W., et al. (2016). Primary production in the Chukchi Sea with potential effects of freshwater content. *Biogeosciences* 13 (3), 737–749. doi: 10.5194/bg-13-737-2016

Zhang, X., He, J., Zhang, J., Polyakov, I., Gerdes, R., Inoue, J., et al. (2013). Enhanced poleward moisture transport and amplified northern high-latitude wetting trend. *Nat. Climate Change* 3 (1), 47–51. doi: 10.1038/nclimate1631

Zhang, T., Wang, R., Xiao, W., Polyak, L., Astakhov, A., Dong, L., et al. (2021). Characteristics of terrigenous components of amerasian Arctic Ocean surface sediments: Implications for reconstructing provenance and transport modes. *Mar. Geology* 437, 106497. doi: 10.1016/j.margeo.2021.106497

Zhang, W., Yu, X., Wang, W., Liu, Y., Ye, L., Bian, Y., et al. (2018). Records of organic carbon and total nitrogen for environmental change in the Chukchi Sea during the past 100 years. *Marine Geology & Quaternary Geology* 38(2), 13–24 (in Chinese with English abstract). doi: 10.16562/j.cnki.0256-1492.2018.02.002

Zhuang, Y., Jin, H., Li, H., Chen, J., Lin, L., Bai, Y., et al. (2016). Pacific inflow control on phytoplankton community in the Eastern Chukchi Shelf during summer. *Continental Shelf Res.* 129, 23–32. doi: 10.1016/j.csr.2016.09.010